

Spring 1-1-2018

Chemical Characterization of Natural Soiling on Solar Panel Glass Covers in an Urban Environment

Faisal Ali Alamri

University of Colorado at Boulder, faal2757@Colorado.edu

Follow this and additional works at: https://scholar.colorado.edu/mcen_gradetds



Part of the [Environmental Engineering Commons](#), and the [Mechanical Engineering Commons](#)

Recommended Citation

Alamri, Faisal Ali, "Chemical Characterization of Natural Soiling on Solar Panel Glass Covers in an Urban Environment" (2018).
Mechanical Engineering Graduate Theses & Dissertations. 187.
https://scholar.colorado.edu/mcen_gradetds/187

This Thesis is brought to you for free and open access by Mechanical Engineering at CU Scholar. It has been accepted for inclusion in Mechanical Engineering Graduate Theses & Dissertations by an authorized administrator of CU Scholar. For more information, please contact cuscholaradmin@colorado.edu.

Chemical characterization of natural soiling on solar panel glass covers in an urban environment

By

Faisal A. Alamri

B.S., King Fahd University of Petroleum and Minerals, 2014

A thesis submitted to the
Faculty of the Graduate School of the
University of Colorado in partial fulfillment
of the requirements for the degree of
Master of Science
Department of Mechanical Engineering
2018

This thesis entitled:
Chemical characterization of natural soiling on solar panel glass covers in an urban environment
Written by Faisal A. Alamri
has been approved for the Department of Mechanical Engineering

Dr. Marina E. Vance

Prof. Michael P. Hannigan

Date_____

The final copy of this thesis has been examined by the signatories and we find that both the content and the form meet acceptable presentation standards of scholarly work in the above mentioned discipline.

Alamri, Faisal A. (M.S., Mechanical Engineering)

Chemical characterization of natural soiling on solar panel glass covers in an urban environment

Thesis directed by Dr. Marina E. Vance

Photovoltaic (PV) systems are an important source of renewable energy in the United States and the world. As PV systems become more commonly used in urban environments, PV soiling by urban air pollution must be investigated. This study investigates the effects of aging and urban air pollutant deposition on multiple nanotechnology-enabled coating materials, described as “self-cleaning”, “hydrophilic”, and “hydrophobic”, applied onto glass panels that were exposed to natural soiling at different tilt angles (30°, 45°, 60°). Light meter measurements in the field showed no significant differences among samples. UV-Vis analysis showed that new self-cleaning coating started with 3.9% lower transmittance values than other samples, but after 4 months of natural aging, the hydrophobic sample performed ~ 2% better than others. XPS results showed that although freshly-coated samples had distinct elemental compositions, those compositions became similar after 4 months of field deployment. Results from this study will help elucidate the reliability of additive coatings for the protection of PV systems in urban environments and bring insights into the chemical and physical processes associated with urban PV aging.

Dedication

This thesis is dedicated to my parents Ali Alamri and Mohrah Alamri whose love and support helped me accomplish my goals.

Acknowledgments

I would like to thank my advisor, Dr. Marina E. Vance, for her research guidance, support, and patience throughout this journey. Also, I am grateful to the Colorado Department of Health and Environment for housing the soiling station at their I-25 Globeville air quality monitoring site. I would like to thank the Virginia Tech National Center for Earth and Environmental Nanotechnology Infrastructure (NanoEarth), a member of the National Nanotechnology Coordinated Infrastructure (NNCI), supported by NSF (ECCS 1542100) for their collaboration. Also, thanks to King Abdulaziz City for Technology and Science for providing salary support. I would like to express my gratitude to my lab mates, Sarah, Zachary, Sameer, and Sumit for their valuable comments.

Finally, I would like to thank my wonderful parents for believing in me and for their continuous support, my amazing wife, Bayan, for always being there for me and my cheerful baby boy, Ali, for his smile that brings joy to my life.

Mother and father, I would not be who I am today if it was not for you, thank you.

Table of Contents

Chapter 1

Introduction.....	1
Materials and Methods.....	5
Glass samples and coatings.....	5
Field deployment.....	6
Light transmittance measurements.....	6
Surface characterization.....	7
Air quality and weather monitoring.....	7
Results and Discussion.....	8
Light transmittance spectrum after deployment.....	8
Light transmittance ratios (LTR) during deployment and the effect of rain.....	9
Effects of wind and particulate matter concentrations (PM _{2.5} and PM ₁₀).....	11
Multiple Linear Regression Analysis.....	12
Surface Chemistry.....	15
Conclusions.....	17
Bibliography.....	19
Supplemental Information.....	23

List of Tables

Table 1. Description of number, coating type, and tilt angle of small (2×2 cm) and large (10×10 cm) glass samples used in this study.....	5
Table 2. Average transmittance (%) for new and three-month-old coated samples (average values reported with standard deviation values)	9
Table 3. R^2 values for each linear regression analysis between light transmittance.....	13
Table 4. Elemental information of the dust layer on each sample (aged and new coated samples).	15

List of Figures

Figure 1. Drops of water over glass slides, uncoated (a), hydrophilic (b), self-cleaning (c), and hydrophobic (d) products.....	6
Figure 2. Light transmittance in the 350 – 700 nm range for new coated glass samples and samples exposed to natural soiling for four months.	8
Figure 3. Time series showing weekly LTR values for all glass samples (a) and daily precipitation rates (b) throughout the 4-month deployment period.	10
Figure 4. Wind speed and direction rose showing a range of the wind speed from 0 – 20 mph.	11
Figure 5. PM _{2.5} rose for concentration ranging from 0 to 20 $\mu\text{g m}^{-3}$ (a) and PM ₁₀ concentration rose for concentrations ranging from 0 to 200 $\mu\text{g m}^{-3}$ (b).	12

Chapter 1

Introduction

More energy from sunlight strikes the Earth in one hour than all energy consumed by humans in an entire year [1]. With a growing interest in carbon-free energy production, solar electricity or photovoltaic (PV) technology is gaining attention as a potentially popular approach for sustainable energy generation [2]. PV panels have been implemented on different scales so far, from household to large-scale use, such as in industrial and power plant applications, due to their many advantages including a lack of moving parts and the fact that no air pollution or greenhouse gases (GHG) are emitted during direct use [3], [4].

Due to advantages in both technological and economical aspects, solar photovoltaic (PV) industry has been expanding and developing rapidly worldwide. However, many significant factors limit the performance of solar conversion efficiency of PV modules. The power output delivered from photovoltaic modules depends heavily on the amount of solar irradiance that reaches the solar cells and eventually gets converted to electricity. Thus, light transmittance is an essential element playing a role in PV performance [3], [4]. Large PV installations are commonly located in areas of high solar radiation intensity such as deserts, where the weather is windy and dry [4]. One downside of such locations is the high potential for surface dust accumulation [4]. Smaller-scale PV installations, however, may take place in a variety of weather and air pollution conditions.

The deposition of ambient particulate matter (PM) onto the surface of PV modules—also referred to as dust accumulation or natural soiling—has been a focus of attention and has been studied in different environments and conditions and can cause significant losses in solar input [5], [6]. The extent of dust soiling on PV module performance has been investigated through controlled laboratory studies [7], [8] and field studies [5], [9].

A laboratory study by Mohammad et al. found that the deposition of atmospheric dust particles with a mean diameter of 80 μm reduced the short-circuit current by 80% as the accumulation level reached 250 g m^{-2} [7]. Another laboratory study performed by Jiang et al. found a 26% reduction of output efficiency when dust deposition density increased from 0 to 22 g m^{-2} [8]. Another study examined the effect of urban air pollutants (i.e. red soil, carbonaceous fly-ash, and limestone particles) on PV panels under the same environmental conditions inside the laboratory, as the study resulted in a reduction in the output energy by 7.5%, 4% and 2.3% for red soil, limestone, and ash, respectively [10].

Field studies have the potential to directly investigate air pollutants based on solar panel location. Commonly, PV soiling dust in urban areas is formed by heavy metals originating from three primary sources: automobile activities, weathered materials, and industries [5]. A field study by Elminir et al. was performed in hot, dry, and dusty weather, and resulted in a noticeable decrease in the output power (about 17.4% per month) with panels installed at a 45° tilt angle [5]. On the other hand, a study by Boyle et al. performed in a semi-arid environment (Commerce City, CO) found a transmission loss of 0.09% with a mass accumulation of 1.5 g/m^2 [9].

PM deposition in arid environments is not the only reason for soiling losses. Urban environments could have an impact on the performance of photovoltaic systems, especially during the dry season [11]. Kimber et al. examined PV energy loss in different urban locations in southern

California and found an efficiency reduction of 0.2% per day as a result of both particulate matter accumulation and dirt [11]. Another study examined the effect of urban air pollutants (i.e. red soil, carbonaceous fly-ash, and limestone particles) on PV panels under the same environmental conditions inside the laboratory, as the study resulted in a reduction in the output energy by 7.5%, 4% and 2.3% for red soil, limestone, and ash, respectively [10].

Another factor influencing the light transmittance of solar panel glass is their tilt angle. Different solar panel glass covers have been studied with varying tilt angles 0°, 15°, 30°, 45°, 60°, 75°, and 90° resulting in a dust deposition density reduced from 15.84 to 4.48 g/m² as tilt angles increases, and the corresponding transmittance diminishes by 52.54 to 12.38%, respectively [5]. A study performed in Egypt examined the effect of tilt angle and found that horizontal plates were the most easily contaminated with both fine and coarse dust particles, and vertical plates were the least contaminated [6]. Another study was done in Tehran and found that as the tilt angle decreases, pollen and air contaminants have a higher chance of accumulating on PV surfaces and are harder to be washed away by rainfall [12].

Furthermore, wind speed has a critical correlation with dust accumulation rates and the sedimentological structure of dust coatings on solar panels. In a wind tunnel study, higher wind speeds were associated with higher light transmittance values as a result of lower dust accumulation rates and different sedimentological structures of dust coatings [13].

Light transmittance can vary not only with dust deposition, but also on the presence and type of coatings used on PV glass cover plates. Nowadays, many types of glass coatings can be used to improve glass panel efficiency. These coatings can confer novel properties or enhancement to the glass, such as anti-reflective, anti-fouling, and self-cleaning. Anti-reflective coatings are especially

popular for improving the light transmittance of PV covers [14]. Anti-reflective coatings have become a vital feature of high-efficiency silicon solar cells [15]. Silicon dioxide (SiO_2) anti-reflective coatings are currently used commercially and have attracted attention due to their enhancement in light transmittance as a result of their low surface scattering [16]. A SiO_2 coating with 89 nm in thickness has been shown to diffuse light reflectance by 5% for 550-nm wavelength light [17]. Another study by Tsui et al. has shown a fixed light reflectance of 5% of the total light incidence with Anti-reflective nano-cone covering, as the tilt angle was changed from 0° to 60° [18].

Coating materials are widely used and the global market for anti-reflective coatings accounted for \$3.53 billion in 2016 and is expected to reach \$5.71 billion by 2022 [19]. Currently, the North American market share of anti-reflective coatings is the largest across the globe and there is an increasing rate of adoption of anti-reflective coatings in consumer electric devices (such as tablets, smartphones, cameras, etc.) [19]. Brazil and Argentina jointly accounted for approximately 50% of the consumption of optical coatings in Latin America as the region has witnessed a rapid increase in the investment and the revenue is expected to reach \$354 million in 2022 [20].

The purpose of this study was to examine the effects of weather and air pollution on the light transmittance of PV panels enhanced by the application of multiple nanotechnology-enabled coating products. Specific objectives were to investigate the influence of certain coating materials and their natural aging and soiling on light transmittance, as well the impact of tilt angle on dust deposition. Lastly, the effects of weather conditions, such as rainfall, wind direction and wind speed, and relative humidity, on light transmittance were also investigated.

Materials and Methods

Glass samples and coatings

Samples of extra clear low-iron float glass (Pilkington Optiwhite “S”) with 3.2 mm thickness were used for this study. This type of glass is commonly used for PV applications [21], [22]. Glass samples were cut into eight 10 cm × 10 cm slides for light transmittance measurements and into 32 2 cm × 2 cm for surface chemistry analysis. Table 1, shows further details of experimental samples.

Table 1. Description of number, coating type, and tilt angle of small (2 × 2 cm) and large (10 × 10 cm) glass samples used in this study.

Tilt angle	Coating type			Uncoated (control)
	Self-cleaning	Hydrophobic	Hydrophilic	
30°	5 small	5 small	5 small	5 small
	1 large	1 large	1 large	1 large
45°	3 small	0	0	3 small
	1 large			1 large
60°	3 small	0	0	3 small
	1 large			1 large

Three types of commercially-available coating products were applied to triplicate glass slides, each advertising to confer distinct surface properties: self-cleaning (Balconano, Balcony Systems Solutions Ltd), hydrophobic (Rain-X, ITW Global Brands), and hydrophilic (P100, Joninn Inc). These products can be used for a number of applications, including glass surfaces. Differences in the three coating materials can be visualized by the contact angle of water droplets as seen in

Figure 1. The sharpness of the water contact angle decreases as the coating material tends to exhibit hydrophobic characteristics (less than 90°) and increases as the coating material tend to exhibit hydrophilic characteristics [23].

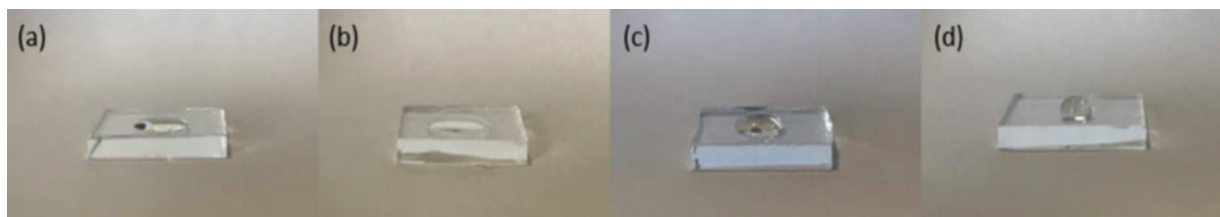


Figure 1. Drops of water over glass slides, uncoated (a), hydrophilic (b), self-cleaning (c), and hydrophobic (d) products.

Field deployment

Samples were affixed to an unpainted wooden platform (Figure S1) was built to house glass samples at three tilt angles: 30° , 45° , and 60° . This platform was deployed at one of the Colorado Department of Public Health and Environment (CDPHE) air quality monitoring stations in the city of Denver, CO (station ID: I-25 Globeville), located adjacent to a 14-lane interstate highway. Samples were deployed on June 16th, 2018 and removed on October 11th, 2018 for a ~four month deployment period.

Light transmittance measurements

Light transmittance through the large glass slides was measured on-site once per week using a solar power meter with spectral response of 400 to 1000 nm and 0.1 W m^{-2} resolution (TES 132, TES Corp.). Light transmittance ratios (LTR) were calculated as the ratio of solar power radiation

measured under each glass sample and a direct solar power measurement with no glass. Both measurements were taken within one minute of each other and performed in triplicate.

After four months of exposure to natural aging and soiling (June – October 2018), one sample from each coating at the 30° tilt angle was removed from the setup and was analyzed for light transmittance of 200-800 nm range at room temperature using a single-beam UV–vis-NIR spectrophotometer (Cary 5000). The system was zero/baseline corrected when the beam passes through a 5-mm pinhole in the solid sample holder. Each sample was measured three times with different beam pass locations.

Surface characterization

After four months of deployment, one small sample from each coating at 30° tilt angle was removed from the setup and also analyzed using X-ray Photoelectron Spectroscopy (XPS, PHI Quantera SXM). Fresh coatings were applied to additional samples to draw a direct comparison between new and aged samples.

Air quality and weather monitoring

Air quality monitoring data was obtained from CDPHE for this specific site and included hourly mass concentrations of PM_{2.5} and PM₁₀. Some weather parameters are also measured at this station, including hourly monitoring for wind speed, wind direction, relative humidity, and temperature. Daily precipitation data was retrieved from the PRISM climate group at Oregon State University [24].

Results and Discussion

Light transmittance spectrum after deployment

Figure 2, below, shows the visible light transmittance spectrum for new samples and those that had been aged for four months.

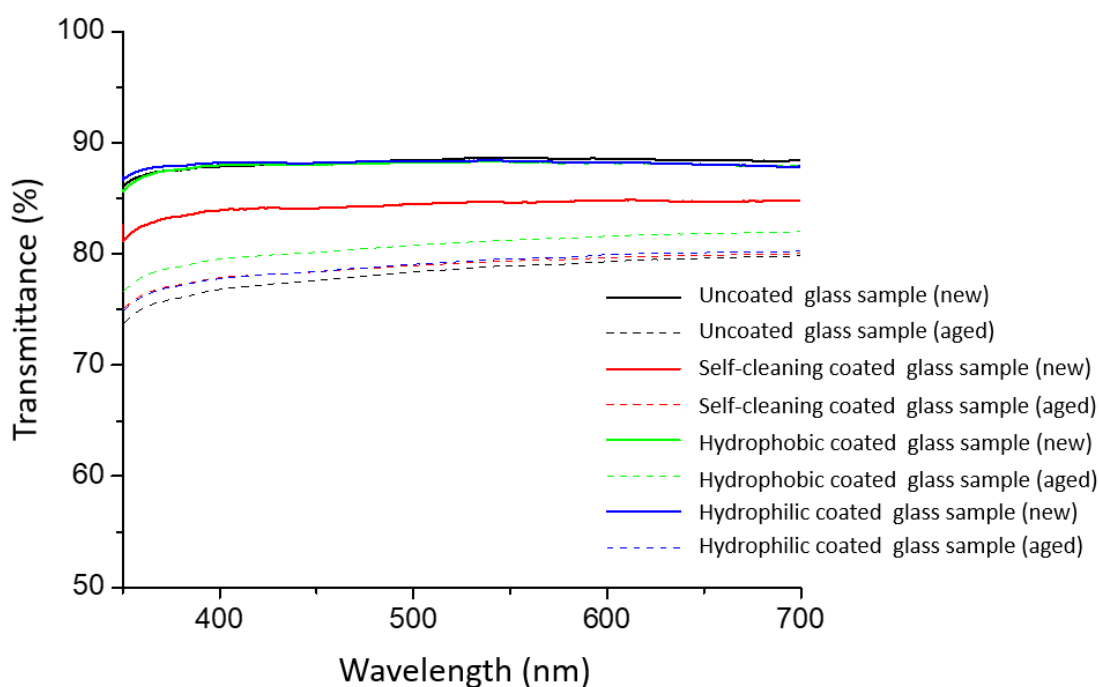


Figure 2. Light transmittance in the 350 – 700 nm range for new coated glass samples and samples exposed to natural soiling for four months.

The new, bare glass (uncoated control) sample exhibited a high light transmittance ($88.2 \pm 0.4\%$, Table 3) that was homogeneous for the visible light spectrum. This value is 3.4% lower than the transmittance informed by the manufacturer [22], and the transmittance observed using the wavelength-integrated solar power meter. The “new” hydrophobic and hydrophilic coatings had similar light transmittance for new samples and the self-cleaning coating started with 3.9% lower

transmittance values, which is statistically significant ($p < 0.01$ according to ANOVA tests). After four months of natural aging and soiling, the uncoated sample had statistically significantly worse performance than self-cleaning, hydrophilic, and hydrophobic samples ($p < 0.01$). The self-cleaning sample continued to perform worse than the hydrophilic and hydrophobic samples. The hydrophobic sample performed $\sim 2\%$ better than other samples ($p < 0.005$ according to ANOVA test). Average light transmittance values are reported in Table 2.

Table 2. Average transmittance (%) for new and four-month-old coated samples (average values reported with standard deviation values)

Coating type	Average transmittance (%) over 350 – 700 nm	
	New	Aged
Uncoated (control)	88.2 \pm 0.4	78.3 \pm 3.0
Self-cleaning	84.3 \pm 0.7	78.9 \pm 1.9
Hydrophobic	88.0 \pm 0.3	80.7 \pm 0.9
Hydrophilic	88.1 \pm 0.6	79.0 \pm 0.8

Light transmittance ratios (LTR) during deployment and the effect of rain

Figure 3, below, shows a time series of the light transmittance ratio measurements performed on site during the 4-month deployment period as well as daily precipitation data. Figure S2, in the supplemental file, shows individual light transmittance values for each coating and tilt angle.

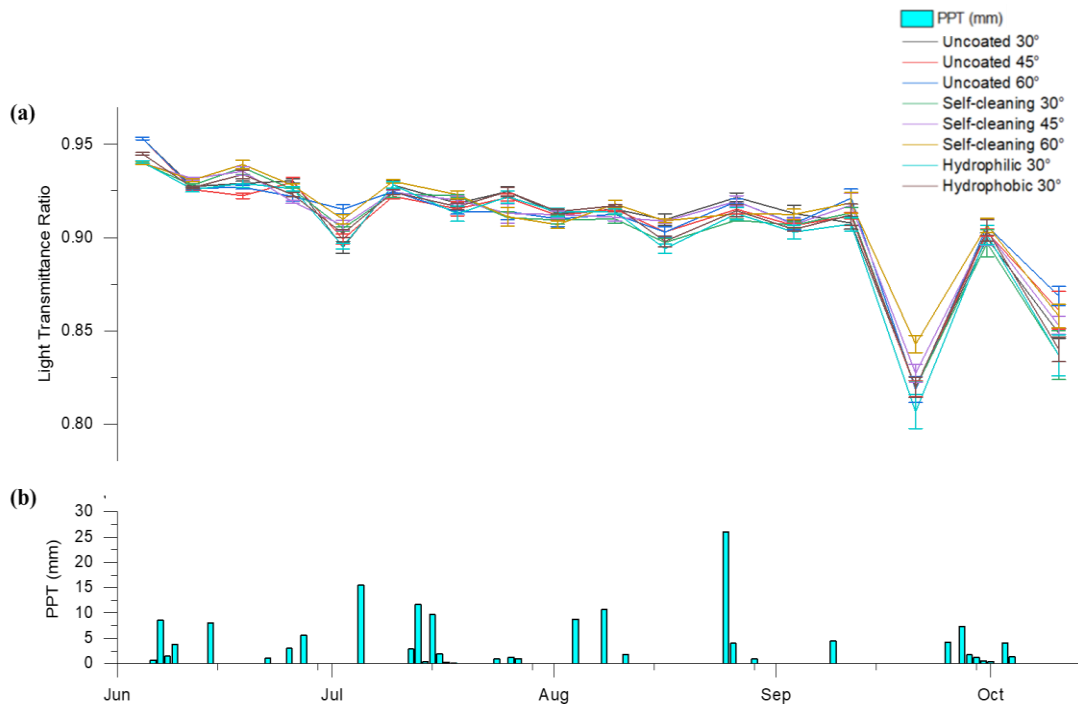


Figure 3. Time series showing weekly LTR values for all glass samples (a) and daily precipitation rates (b) throughout the 4-month deployment period.

The time series in Figure 3 shows that there is no significant difference between each coating material or tilt angle ($p > 0.05$ according to ANOVA tests). In seven out of the 16 weeks in which rainfall occurred, the values of the LTR for glass samples increased which indicates that rainfall events might have contributed to the removal of dust accumulation on the glass surfaces. However, this is not always the case, as some rainfall events, especially those with < 5 mm total precipitation could have contributed to dust accumulation. Previous studies have found that 5 mm of rainfall can be sufficient enough to clean PV systems [25], [26].

Effects of wind and particulate matter concentrations (PM_{2.5} and PM₁₀)

Field deployment took place directly east of the I-25 highway and west of a residential area which also contained a large construction site. Several train tracks also surround the location, primarily on the west and south directions. As a result, there are many different PM₁₀ and PM_{2.5} sources from multiple directions as can be seen in Figures 4 and 5.

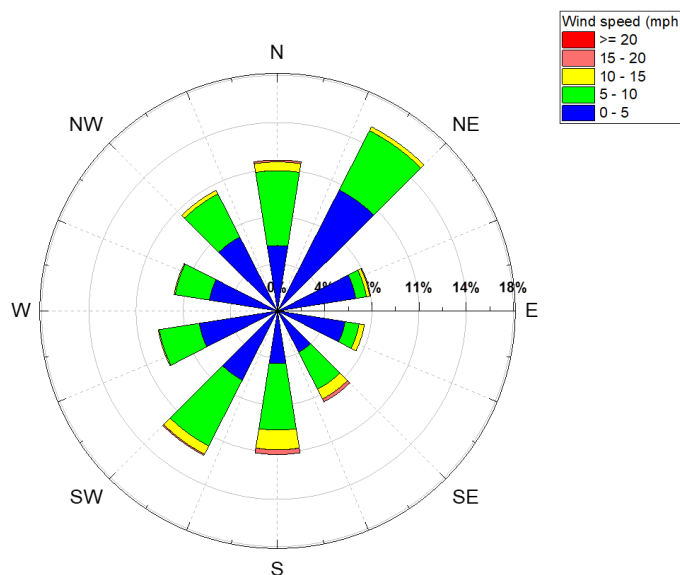


Figure 4. Wind speed and direction rose showing a range of the wind speed from 0 – 20 mph.

Wind from northeast and southwest directions were prevailing at the field site during the period of deployment. Wind speed patterns homogeneously distributed through most directions, although higher wind speeds (> 10 mph) were observed mostly from the north and south directions.

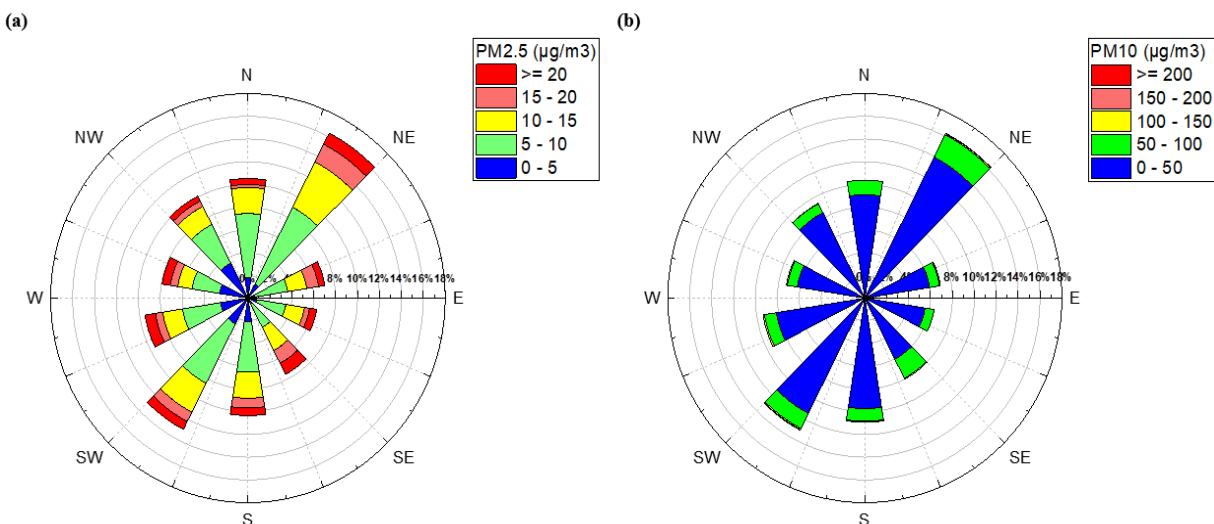


Figure 5. PM_{2.5} rose for concentration ranging from 0 to 20 µg m⁻³ (a) and PM₁₀ concentration rose for concentrations ranging from 0 to 200 µg m⁻³ (b).

Figure 5 shows that PM_{2.5} and PM₁₀ are predominantly carried to the monitoring site from the NE and SW directions because these are the prevailing wind directions at this location. Additionally, there are no evident sources of high concentrations of PM_{2.5} and PM₁₀ linked to a specific wind direction because PM concentrations are well distributed through most directions. Low concentrations of PM_{2.5} (0 – 5 µg/m³) are associated with the western direction, where the I-25 highway is located, and slightly higher PM_{2.5} concentrations are associated with western directions.

Multiple Linear Regression Analysis

The soiling of glass panel surfaces and, thus, their light transmittance, can be affected by many environmental factors such as rainfall, wind speed, PM₁₀ and PM_{2.5}, and relative humidity. In order to better understand the relationships between these environmental parameters and natural soiling, some statistical analyses were performed. For such analyses, weekly light transmittance (LTR) measurements were used to obtain a soiling rate (SR), as shown in Equation 1. A positive

SR value indicates that soiling occurred and a negative SR value indicates that natural cleaning occurred.

$$SR = \frac{LTR_{before} - LTR_{after}}{\text{time period (days)}} \quad (\text{Eq. 1})$$

Natural soiling or cleaning events were considered to be independent from other weeks and combined into a dataset of SR measurements. A simple linear regression analysis was performed to investigate the relationships between each environmental input against the SR output separately. Table 3 shows the R^2 values obtained for each single input against SR. For rainfall, wind speed, and PM concentrations, both the average for each period, and a total sum of measurements during each period were considered. Although a sum of PM concentrations does not have a physical meaning, it is used here as a proxy for the cumulative PM exposure suffered by the samples.

Table 3. R^2 values for each linear regression analysis between light transmittance.

Environmental input		R^2 values against SR
Rainfall	Total sum of period	0.062
	Maximum value observed	0.250
Wind speed	Average of period	0.060
	Maximum value observed	0.016
Relative Humidity (RH)	Maximum value observed	0.072
PM _{2.5}	Total sum of period	0.035
	Maximum value observed	0.024
PM ₁₀	Total sum of period	0.073
	Maximum value observed	0.004

Clearly, no simple relationship was able to approximate the soiling rate values observed, as all R^2 are well below 0.8. The sum of Rainfall yielded the highest R^2 values, although still too low to indicate goodness of fit.

To study the relationship between the soiling rates (SR) and the various environmental inputs concurrently, a multiple linear regression analysis was performed to assess the relationships between all environmental inputs and the soiling rate output. In addition to the total and maximum rainfall values, an additional model was run considering rainfall events as a categorical variable. In this case, rainfall events > 5 mm were treated as “yes” and < 5 mm as “no”. This condition was chosen because 5 mm precipitation is suggested in the literature as a critical amount of rainfall required to clean PV panels [11]. Other categorical variables included the type of coating and tilt angle.

Several model runs were performed using a combination of the variables listed on Table 3 in addition to the type of coating, tilt angle, and rainfall above/below 5 mm. It was observed that the type of coating and tilt angle were not able to explain SR observations ($p = 0.933$ and $p = 0.704$, respectively). Consequently, those two inputs were removed from subsequent analyses and only control (uncoated) samples at 30° tilt angle were used. The model with best fit used the following variables: total amount of rainfall ($p = 0.083$), cumulative PM_{10} ($p = 0.084$), maximum wind speed ($p = 0.083$), and maximum relative humidity ($p = 0.082$), with an R^2 value of 0.67. The same model will be examined as the study continues to measure the LTR over the next eight months to establish better relationships between environmental inputs and the soiling rate. $PM_{2.5}$ was removed from the model as a high multicollinearity between $PM_{2.5}$ and PM_{10} had been found. As a result, an empirical relationship was formulated to find a relationship between the soiling rate (SR) and environmental parameters (Equation 2):

$$\text{Soiling Rate (\% per week)} = -51.5 - 0.200 \times \text{rainfall}_{tot} + 1.087 \times \text{Wind}_{max} + 0.343 \times \text{RH}_{max} + 0.001713 \text{ PM}_{10,tot} \quad (\text{Eq. 2})$$

Surface Chemistry

All glass samples located at the 30° tilt angle were examined by X-ray photoelectron spectroscopy (XPS) to analyze the elemental composition of topmost layer (approximately the 10 nm of the surface) of each sample. Table 4 shows compositional information of the coating and/or dust accumulation on the samples' surfaces for both aged samples and new ones. Figures S3-S10, in the supplemental information file, show specific XPS spectra for all samples.

Table 4. Elemental information of the dust layer on each sample (aged and new coated samples).

Sample		Detected Elemental Species (%)						
		C	O	F	Sn	Si	Ca	N
Uncoated (control)	new	35.8	43.8	-	-	20.4	-	-
	aged	35.8	47.9	-	1.6	13.7	0.4	0.5
Self-cleaning	new	21	31.4	32.5	-	15.1	-	-
	aged	42	42	1.7	1.1	13.2	-	-
Hydrophilic	new	78.1	15.4	-	-	3.1	-	3.4
	aged	38.7	46.6	-	1.2	12.2	0.6	0.5
Hydrophobic	new	22.1	50	-	-	27.9	-	-
	aged	41.2	44	-	1.2	11.7	1	0.8

The new, control sample indicates an organic layer that is thought to cover all surfaces [27], resulting in 36% elemental concentration of carbon. The ratio of oxygen to silicon (2.15) is indicative of the 2:1 ratio that is expected for glass (silicon dioxide, SiO₂). The control sample

seems to have oxidized upon aging by gaining 20% of oxygen in relation to the expected 2:1 silicon-to-oxygen ratio. The relative concentration of carbon on the surface remained the same.

The self-cleaning sample also started a ~ 2:1 silicon-to-oxygen ratio (2.1), indicating that those elements were not part of the product composition, unless that also takes place in the form of SiO₂. The new sample had 32.5% fluoride which seems to be associated with the coating product. The amount of carbon on the surface was lower than the control, which would indicate its efficacy as a “self-cleaning sample”, however, after four months of aging, this sample had lost 95% of its fluoride and gained 6% more carbon than the control, indicating that most of the original coating had been removed.

The hydrophilic sample started with a surplus of carbon, oxygen, and nitrogen in relation to the control sample, indicating that this may be the elemental composition of the coating, at a respective elemental ratio of 12:12:1. Upon aging, this sample lost 85% of the nitrogen and both carbon and oxygen elemental concentrations approximated that of the control sample, indicating that most of the coating had been removed.

The new hydrophobic sample had approximately 12% more silicon than the expected composition of SiO₂, indicating that Si could have been part of the coating formulation. This is expected as many hydrophobic materials contain siloxanes (which have a 1:1 silicon-to-oxygen ratio). The amount of carbon on the surface was lower than the control, which would indicate its efficacy, similarly to the self-cleaning-coated sample. However, upon aging, the relative concentrations of carbon, oxygen, and silicon became similar to that of control and other samples, indicating that most of the coating was removed.

Tin (Sn) and calcium (Ca) were found in small amounts (0.4 – 1.6%) in most aged samples but not in new ones, indicating that this element was introduced by natural soiling. All aged samples had similar concentrations of carbon (36 – 42%) and similar O:C ratios (1 – 1.3), indicating that most coatings were removed by natural aging.

Conclusions

This work investigated the effects of urban air pollution on different coating materials applied to glass slides as well as the tilt angle at which these samples were installed. Although coating materials have shown in literature to be an effective solution for reducing soiling and increasing power generation of photovoltaic systems, the results in this study showed otherwise for commercial products, as there was no significant difference between the three coating materials tested according to field measurements of light transmittance. Although field measurements of light transmittance showed no statistically significant differences among samples, wavelength-dependent UV-V is analysis performed in the laboratory showed that new self-cleaning coating started with 3.9% lower transmittance values than other samples. After four months of natural aging, the hydrophobic sample performed ~2% better than others ($p < 0.05$). XPS results showed that although freshly-coated samples had distinct elemental compositions, those compositions became similar after four months of field deployment, indicating either the destruction of the coating, or even accumulation of dust and organic matter throughout the field deployment period. Deployment tilt angles (30°, 45°, and 60°) did not promote significant differences in light transmittance during the deployment period.

Future work in this study includes analyzing Raman spectroscopy and optical image data that has been collected for samples removed after four months of field deployment. Light transmittance data will continue to be collected in the field for eight more month months to complete 12 months of deployment. UV-Vis, XPS, and Raman spectroscopy data will also be collected after 12 months of deployment, as more dust layers are expected to develop on the surface of each sample and lead to differences among tilt angles.

Results from this study will help elucidate the reliability of additive coatings for the protection of PV systems in urban environments and bring insights into the chemical and physical processes associated with urban PV aging.

Bibliography

- [1] N. S. Lewis, "Toward Cost-Effective Solar Energy Use," *Science*, vol. 315, no. 5813, pp. 798–801, Feb. 2007.
- [2] W. Hoffmann, "PV solar electricity industry: Market growth and perspective," *Sol. Energy Mater. Sol. Cells*, vol. 90, no. 18, pp. 3285–3311, Nov. 2006.
- [3] A. Y. Al-Hasan, "A new correlation for direct beam solar radiation received by photovoltaic panel with sand dust accumulated on its surface," *Sol. Energy*, vol. 63, no. 5, pp. 323–333, Nov. 1998.
- [4] M. Mani and R. Pillai, "Impact of dust on solar photovoltaic (PV) performance: Research status, challenges and recommendations," *Renew. Sustain. Energy Rev.*, vol. 14, no. 9, pp. 3124–3131, Dec. 2010.
- [5] H. K. Elminir, A. E. Ghitas, R. H. Hamid, F. El-Hussainy, M. M. Beheary, and K. M. Abdel-Moneim, "Effect of dust on the transparent cover of solar collectors," *Energy Convers. Manag.*, vol. 47, no. 18, pp. 3192–3203, Nov. 2006.
- [6] A. A. Hegazy, "Effect of dust accumulation on solar transmittance through glass covers of plate-type collectors," *Renew. Energy*, vol. 22, no. 4, pp. 525–540, Apr. 2001.
- [7] M. S. El-Shobokshy and F. M. Hussein, "Degradation of photovoltaic cell performance due to dust deposition on to its surface," *Renew. Energy*, vol. 3, no. 6, pp. 585–590, Sep. 1993.
- [8] H. Jiang, L. Lu, and K. Sun, "Experimental investigation of the impact of airborne dust deposition on the performance of solar photovoltaic (PV) modules," *Atmos. Environ.*, vol. 45, no. 25, pp. 4299–4304, Aug. 2011.
- [9] L. Boyle, H. Flinchbaugh, and M. Hannigan, "Impact of natural soiling on the transmission of PV cover plates," in *2013 IEEE 39th Photovoltaic Specialists Conference (PVSC)*, 2013, pp. 3276–3278.
- [10] "Systematic experimental study of the pollution deposition impact on the energy yield of photovoltaic installations - ScienceDirect." [Online]. Available:

<https://www.sciencedirect.com/science/article/pii/S0960148111001182>. [Accessed: 07-Oct-2018].

- [11] A. Kimber, L. Mitchell, S. Nogradi, and H. Wenger, "The Effect of Soiling on Large Grid-Connected Photovoltaic Systems in California and the Southwest Region of the United States," in *2006 IEEE 4th World Conference on Photovoltaic Energy Conference*, 2006, vol. 2, pp. 2391–2395.
- [12] E. Asl-Soleimani, S. Farhangi, and M. S. Zabihi, "The effect of tilt angle, air pollution on performance of photovoltaic systems in Tehran," *Renew. Energy*, vol. 24, no. 3, pp. 459–468, Nov. 2001.
- [13] D. Goossens and E. Van Kerschaever, "Aeolian dust deposition on photovoltaic solar cells: the effects of wind velocity and airborne dust concentration on cell performance," *Sol. Energy*, vol. 66, no. 4, pp. 277–289, Jul. 1999.
- [14] H. Kumar Raut, V. Anand Ganesh, A. Sreekumaran Nair, and S. Ramakrishna, "Anti-reflective coatings: A critical, in-depth review," *Energy Environ. Sci.*, vol. 4, no. 10, pp. 3779–3804, 2011.
- [15] M. A. Green, "High Efficiency Silicon Solar Cells," in *Seventh E.C. Photovoltaic Solar Energy Conference*, Springer, Dordrecht, 1987, pp. 681–687.
- [16] D. T. Carpenter, C. S. Wood, O. Lyngnes, and N. G. Traggis, "Ultra low absorption glasses and optical coatings for reduced thermal focus shift in high power optics," in *High Power Laser Materials Processing: Lasers, Beam Delivery, Diagnostics, and Applications*, 2012, vol. 8239, p. 82390Y.
- [17] Ö. Kesmez, H. Erdem Çamurlu, E. Burunkaya, and E. Arpaç, "Sol-gel preparation and characterization of anti-reflective and self-cleaning SiO₂-TiO₂ double-layer nanometric films," *Sol. Energy Mater. Sol. Cells*, vol. 93, no. 10, pp. 1833–1839, Oct. 2009.
- [18] Tsui Kwong-Hoi *et al.*, "Low-Cost, Flexible, and Self-Cleaning 3D Nanocone Anti-Reflection Films for High-Efficiency Photovoltaics," *Adv. Mater.*, vol. 26, no. 18, pp. 2805–2811, May 2014.

- [19] Z. M. Research, “Global Anti-Reflective Coatings Market will reach USD 5.71 Billion by 2022: Zion Market Research,” *GlobeNewswire News Room*, 14-Feb-2017. [Online]. Available: <http://globenewswire.com/news-release/2017/02/14/916722/0/en/Global-Anti-Reflective-Coatings-Market-will-reach-USD-5-71-Billion-by-2022-Zion-Market-Research.html>. [Accessed: 19-Apr-2018].
- [20] “Optical Coating Market by Type (Antireflection, High Reflection, Transparent Conductive, Filter, Beamsplitter, Electrochromic, and Partial Reflection Coatings), Technology (Vacuum Deposition, E-Beam Evaporation, Sputtering, Ion-Assisted Deposition, and Other Technologies), and End-Use Industry (Electronics & Semiconductor, Military & Defense, Automotive, Construction, Solar, and Medical) - Global Opportunity Analysis and Industry Forecast, 2014-2022,” *Allied Market Research*. [Online]. Available: <https://www.alliedmarketresearch.com/optical-coating-market>. [Accessed: 19-Apr-2018].
- [21] M. A. M. L. de Jesus, J. T. da S. Neto, G. Timò, P. R. P. Paiva, M. S. S. Dantas, and A. de M. Ferreira, “Superhydrophilic self-cleaning surfaces based on TiO₂ and TiO₂/SiO₂ composite films for photovoltaic module cover glass,” *Appl. Adhes. Sci.*, vol. 3, no. 1, p. 5, Mar. 2015.
- [22] “Pilkington Optiwhite™ for Solar applications.” [Online]. Available: <http://www.pilkington.com/en/us/products/product-categories/solar-energy/pilkington-optiwhite-for-solar-applications>. [Accessed: 03-Nov-2018].
- [23] I. P. Parkin and R. G. Palgrave, “Self-cleaning coatings,” *J. Mater. Chem.*, vol. 15, no. 17, pp. 1689–1695, 2005.
- [24] “PRISM Climate Group, Oregon State U.” [Online]. Available: <http://www.prism.oregonstate.edu/explorer/>. [Accessed: 04-Nov-2018].
- [25] R. Hammond, D. Srinivasan, A. Harris, K. Whitfield, and J. Wohlgemuth, “Effects of soiling on PV module and radiometer performance,” in *Conference Record of the Twenty Sixth IEEE Photovoltaic Specialists Conference - 1997*, 1997, pp. 1121–1124.
- [26] M. García, L. Marroyo, E. Lorenzo, and M. Pérez, “Soiling and other optical losses in solar-tracking PV plants in navarra,” *Prog. Photovolt. Res. Appl.*, vol. 19, no. 2, pp. 211–217, Mar. 2011.

- [27] J. Li *et al.*, “Carbonaceous matter and PBDEs on indoor/outdoor glass window surfaces in Guangzhou and Hong Kong, South China,” *Atmos. Environ.*, vol. 44, no. 27, pp. 3254–3260, Sep. 2010.

Supplemental Information



Figure S1. The wooden frame after installing all the stands for both the small and large glass samples (a); The large and small glass samples after fixing them on the stands (b); The whole wooden frame after placing it on the site (I-25 Globeville) (c).

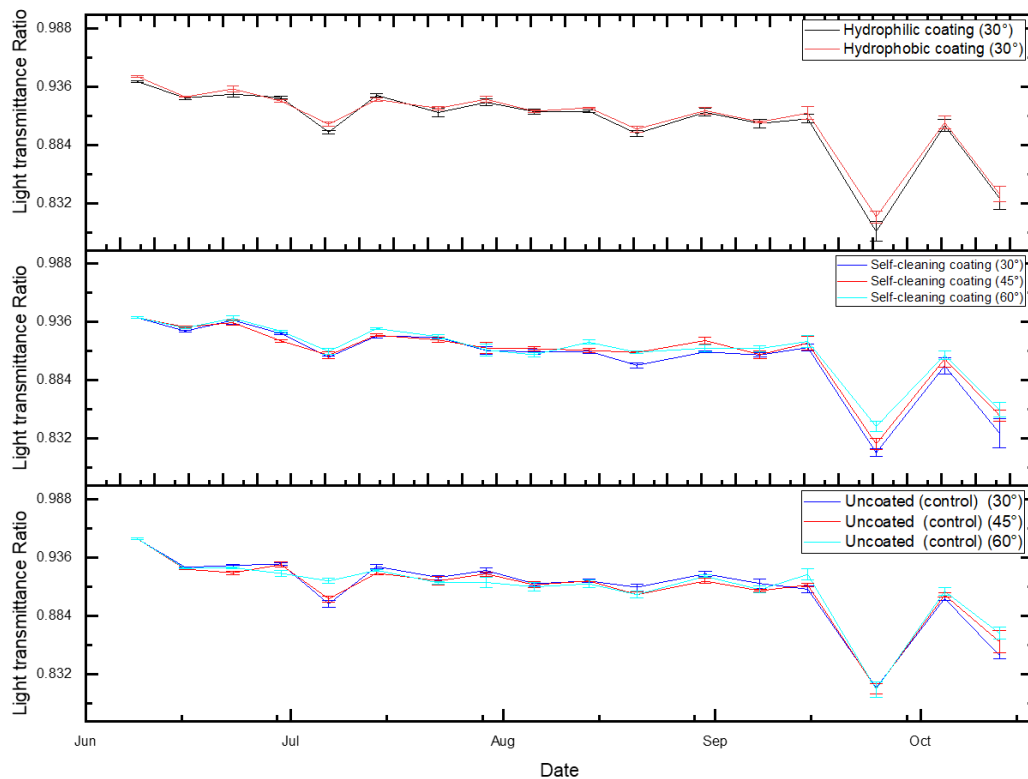


Figure S2. Light transmittance ratio values for all glass samples at each tilt angle (30°, 45°, and 60° tilt angles)

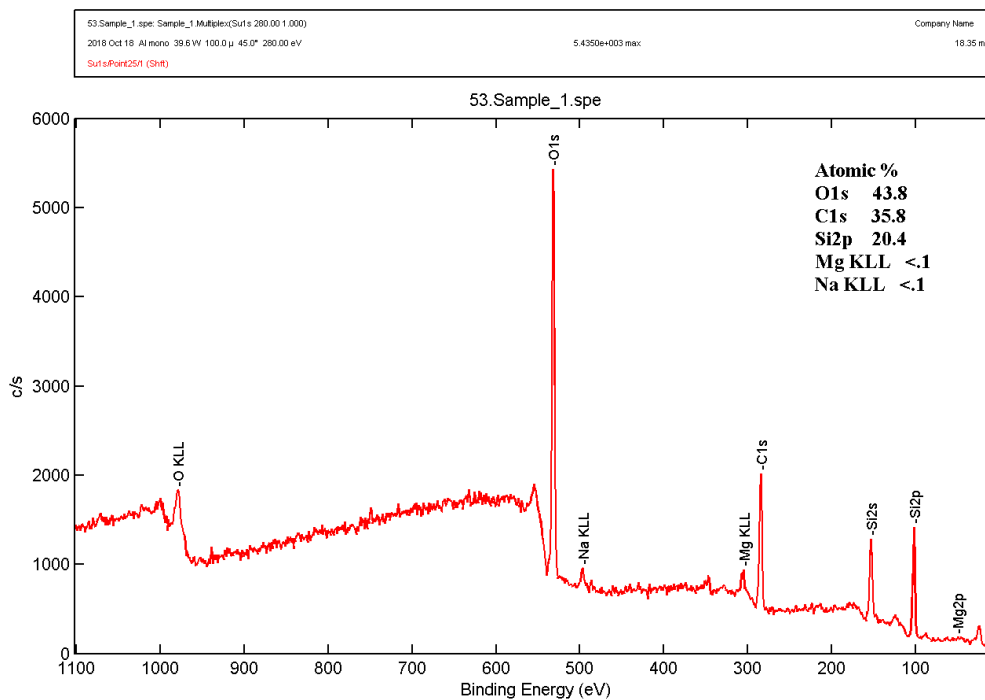


Figure S3. Compositional information of new uncoated sample's surface.

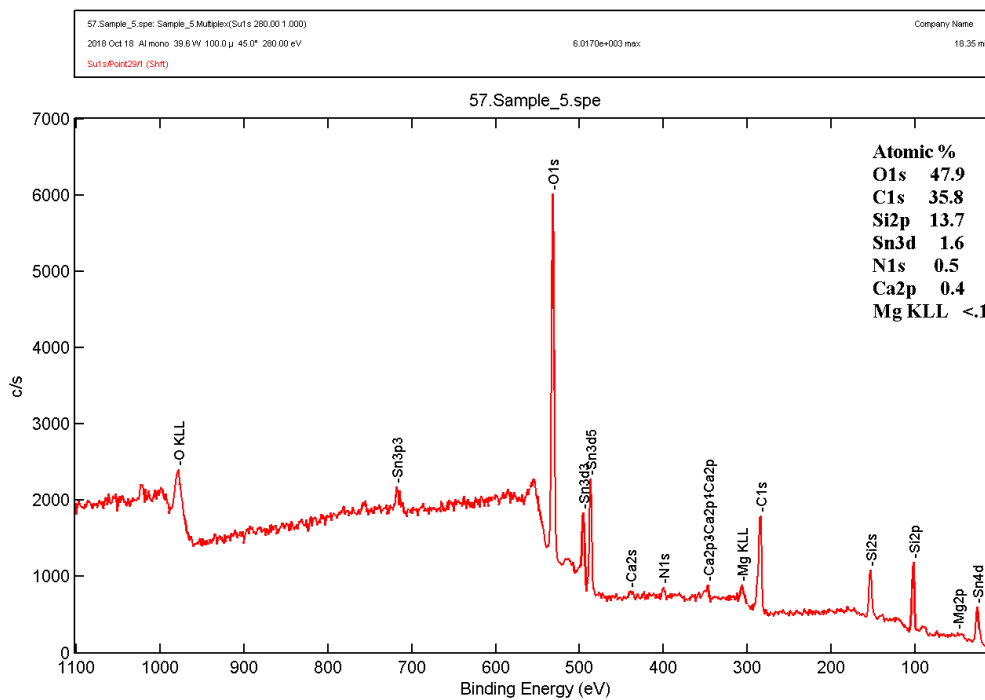


Figure S4. Compositional information of aged uncoated sample's surface.

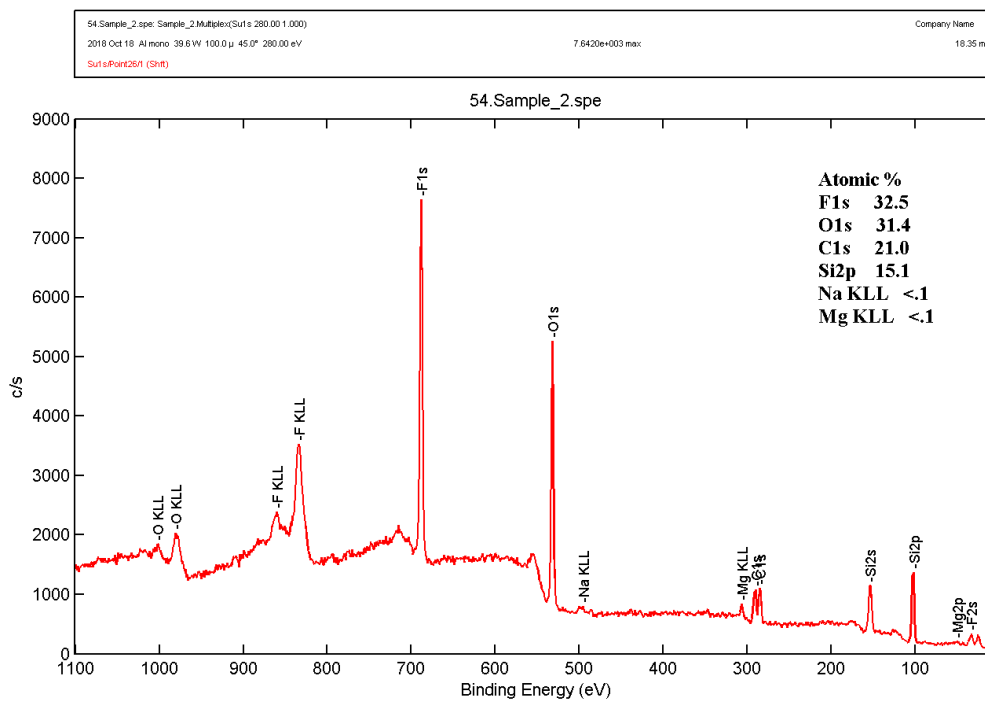


Figure S5. Compositional information of new Self-cleaning coated sample's surface.

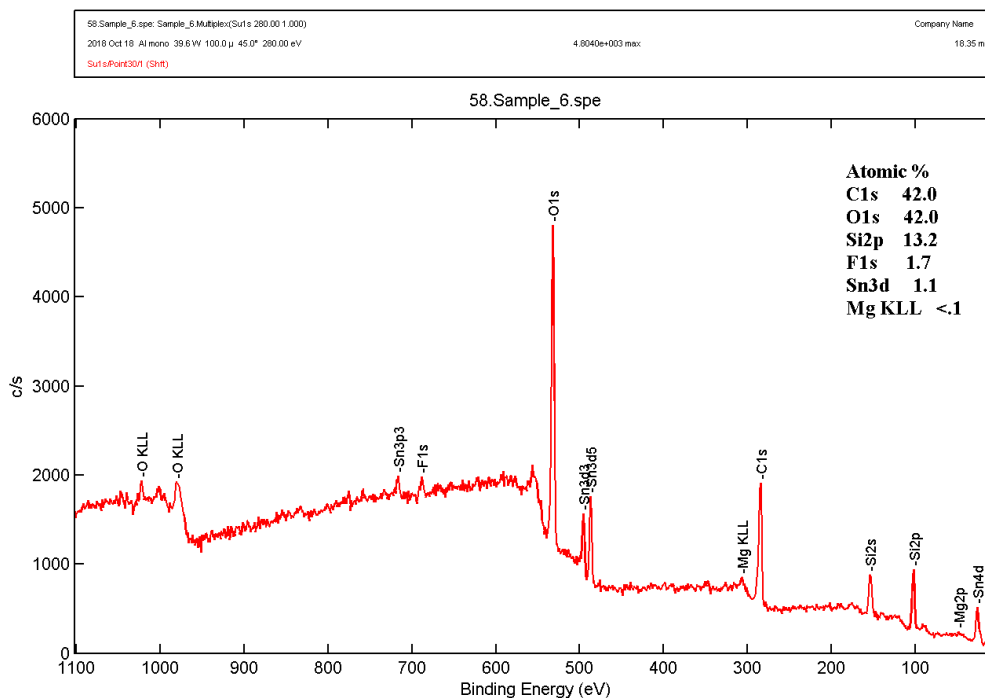


Figure S6. Compositional information of aged Self-cleaning coated sample's surface.

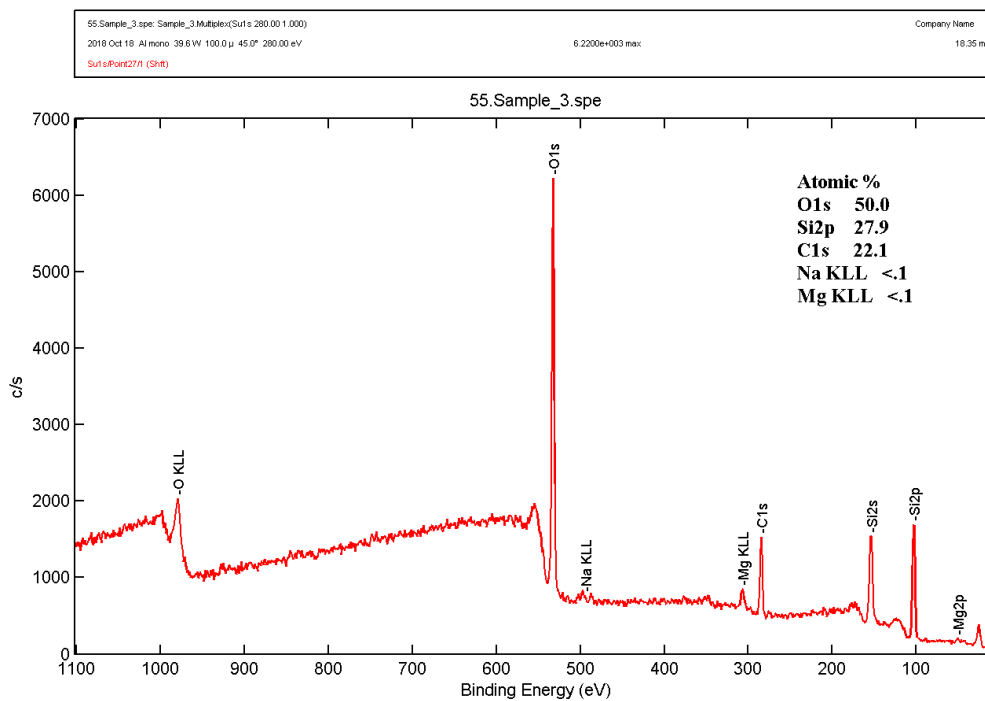


Figure S7. Compositional information of new Hydrophobic coated sample's surface.

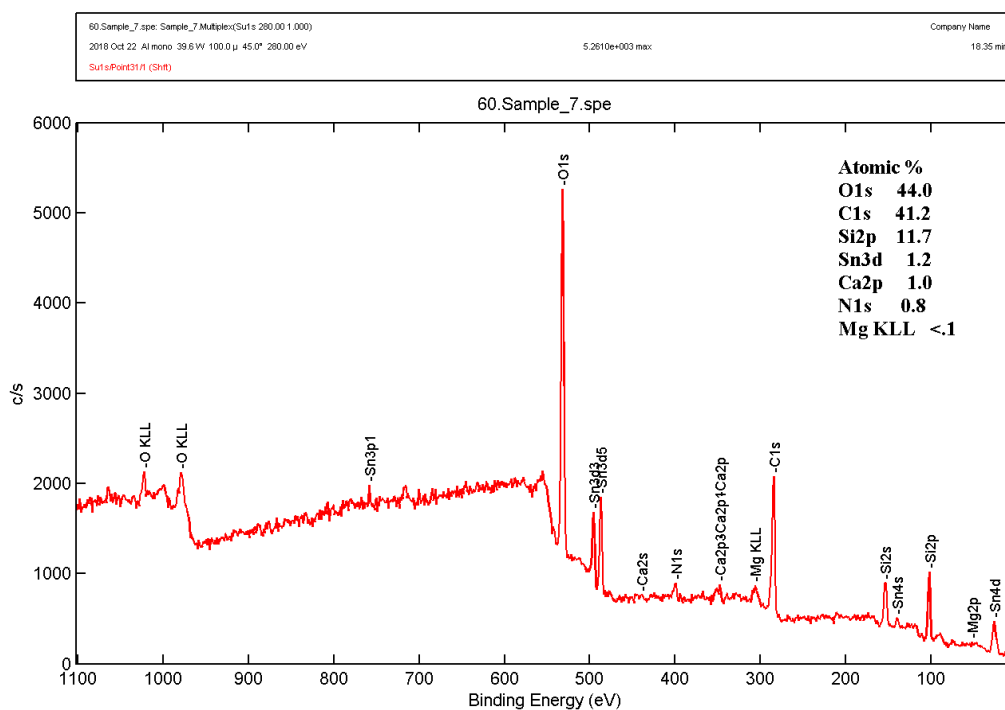


Figure S8. Compositional information of aged Hydrophobic coated sample's surface.

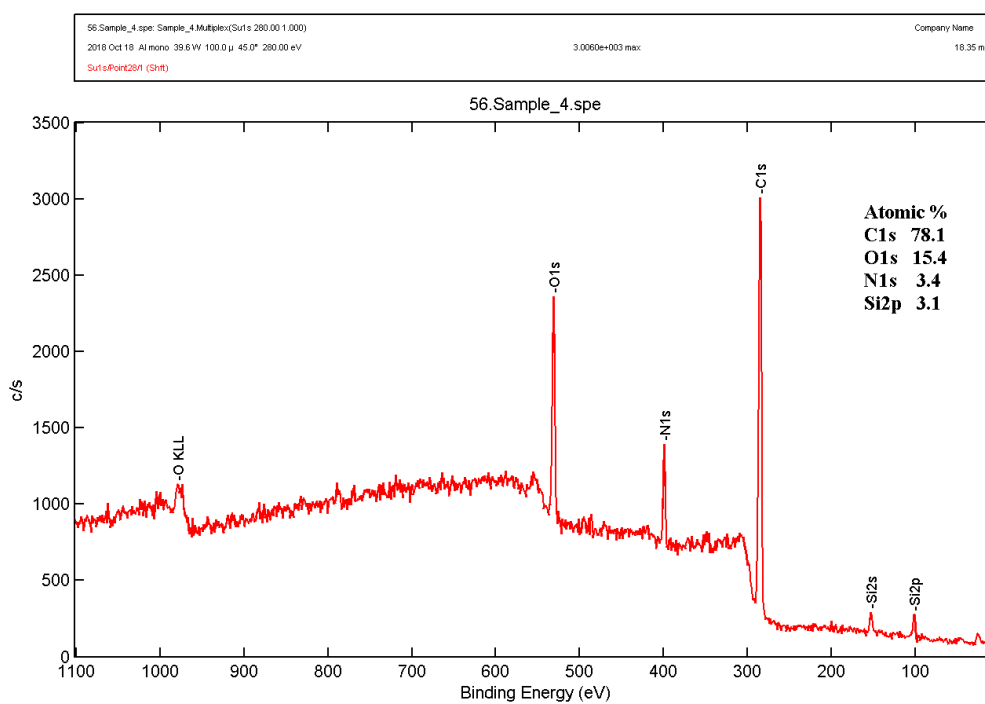


Figure S9. Compositional information of new Hydrophilic coated sample's surface.

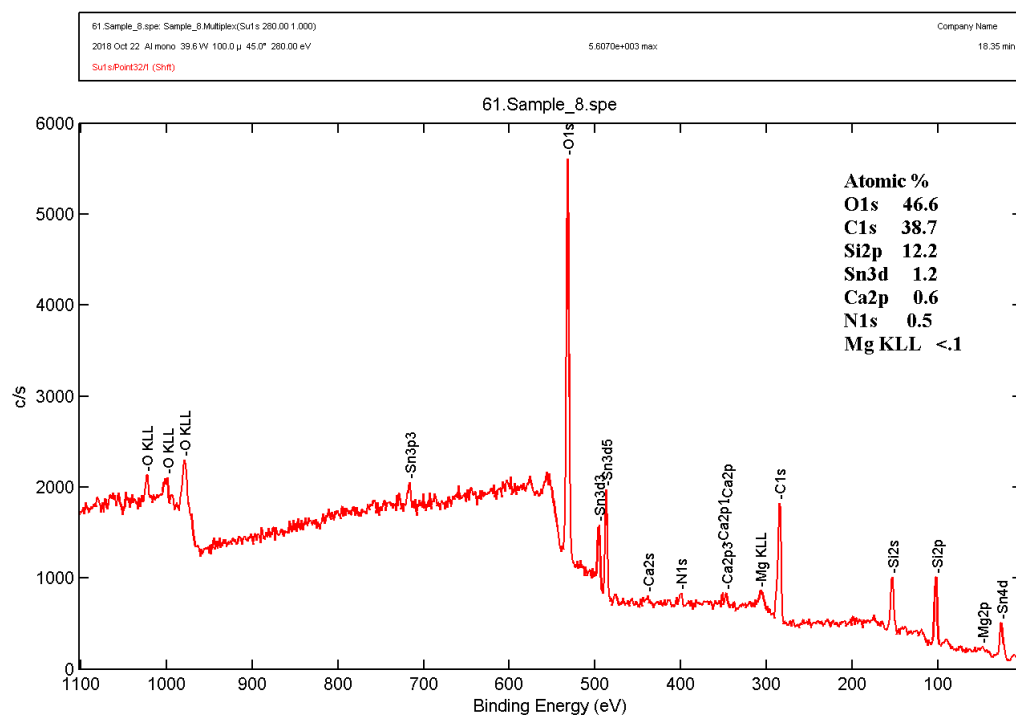


Figure S10. Compositional information of aged Hydrophilic coated sample's surface.